European Journal of Pharmaceutics and Biopharmaceutics 71 (2009) 282–291

Contents lists available at ScienceDirect

European Journal of Pharmaceutics and Biopharmaceutics

journal homepage: www.elsevier.com/locate/ejpb

Nano-salbutamol dry powder inhalation: A new approach for treating broncho-constrictive conditions

Bhavna [a], Farhan Jalees Ahmad [a], Gaurav Mittal [b], Gaurav K. Jain [a], Geena Malhotra [c], Roop K. Khar [a], Aseem Bhatnagar [b,*]

[a] Department of Pharmaceutics, Hamdard University, New Delhi, India
[b] Institute of Nuclear Medicine and Allied Sciences, Delhi, India
[c] Cipla Pharma, Mumbai, India

ARTICLE INFO

Article history:
Received 5 February 2008
Accepted in revised form 30 September 2008
Available online 10 October 2008

Keywords:
Nano-sizing
Anti solvent precipitation
Spray drying
Salbutamol sulphate
Lung deposition
Inhalation

ABSTRACT

Nanoparticle DPI is known to have deeper lung penetration but its clinical utility as a potentially better treatment option needs to be evaluated in the light of higher expected mucociliary movement of the nanoparticles compared to micronized DPI. The objective of this study was to make nano-salbutamol sulphate (SBS) DPI, radiolabel it with Tc-99m using a novel surface labeling methodology, characterize the formulation and assess its in vitro and in vivo deposition in healthy human volunteers to estimate its bioavailability in the target area. Nano-SBS with a mean particle of 60.71 ± 35.99 nm was produced using liquid anti-solvent precipitation method. The drug particles were spherical, pure and crystalline. Anderson cascade impaction showed that blend formulations of Nano-SBS exhibited significantly higher respirable fraction of 45.2% compared to the known behavior of micronized salbutamol sulphate blends. Though the particle size tended to increase due to solid phase interaction after blending with lactose, there was definitive correlation between the radiolabeled and non-radiolabeled forms. In 10 healthy volunteers, lower oropharyngeal depositions (25.3 ± 4.5%) were observed with nano-SBS formulation compared to micronized SBS formulation (58.4 ± 6.1%). Furthermore, Nano-SBS formulations showed nearly 2.3-fold increase in total lung deposition compared to micronized SBS. The in vivo deposition data and the ratio of peripheral to central lung deposition (P/C) of 1.12 ± 0.4 indicate that Nano-SBS is evenly distributed within different lung regions. As demonstrated for SBS, nano-sizing may enhance regional deposition and thus provide an attractive particle engineering option for the development of blend formulations for inhalation delivery.

1. Introduction

Worldwide, more than 300 million people suffer from asthma or COPD [1,2]. It is well known that the local drug delivery of beta-agonists to the respiratory tract offers several advantages over the systemic route in treating broncho-constrictive conditions [3–7]. Compressed air nebulization, metered dose inhalation and dry powder inhalation are now commonly used for targeting drug delivery to the tracheo-bronchial region. However there are several features associated with inhalation therapy that requires improvement. Firstly, deposition in the target area is just 5–15% [8] that reduces further in patients with dyspnoea or mucus plugs in the respiratory pathway. Pharmacological effect of the inhaled drug tends to be short, mostly not more than 1–2 h [9]. In pediatric age group asthma and in advanced COPD small airway involvement are predominant, and inhalation drug delivery systems are not much effective because of poor reach and deposition in small airways. A major portion of the inhaled drug is predominantly swallowed into the esophagus that may lead to acid-induced esophagitis besides drug wastage. Within the inhalation technologies, DPI is favored because of simplicity, ease of use and cost-effectivity. Salbutamol sulphate dry powder inhalation (SBS DPI) is the most important member of this family. Drug particles of SBS in the size range of 5–15 μm have been found therapeutically important because it is this respiratory fraction that coincides with deposition in the target area of trachiobronchial region. Role of micronized SBS DPI is, however, limited to prophylaxis and is used in mild cases. It is not considered potent enough for the treatment of moderate or severe cases [10]. Bronchodilation may be suboptimal or even non-existing because of proximal deposition of drug particles in the presence of mucus, inflammatory fluid, tortuous respiratory pathway and reduced lumen, and poor inspiratory capacity in chronic or severe cases [9]. Clearly, more research is

* Corresponding author. Institute of Nuclear Medicine and Allied Sciences, Brig S K Mazumdar Road, Delhi 110054, India. Tel.: +91 11 23905172; fax: +91 11 23919509.
E-mail address: assem_bhatnagar@indiatimes.com (A. Bhatnagar).

0939-6411/$ - see front matter © 2008 Elsevier B.V. All rights reserved.
doi:10.1016/j.ejpb.2008.09.018

required to make SBS DPI more effective in conditions where it presently has a limited role as a preventive or an adjunct.

It is known that the deposition of inhaled aerosol is related to the particle size; smaller particles tend to travel farther and settle in the deeper and smaller airways [11]. Submicron-sized particles tend to deposit in small bronchi and bronchioles while nanoparticles reach the more peripheral portions of the respiratory tree and alveoli. Such particles are able to negotiate tortuous pathways and mucus plugs better. In the management of asthma and COPD, one of the recent strategies has been the reduction of drug particles size to 1–5 μm level to enhance penetrability, particularly in the presence of inflammatory, obstructive or constrictive factors so that the drug could be directed to the target area in pharmacological dose [12,13]. Several authors have recently demonstrated the changed deposition pattern of the smaller particles using scintigraphy [14]. However, there appears to be a limit for reducing the particle size for enhancing penetration because particles with even lesser size (less than 1 μm, and particularly nanoparticles, less than 400 nm) may not be suitable as delivery system due to mismatched targeting and the fact that inhaled nanoparticles tend to be exhaled significantly [15]. Nanoparticles are solid colloidal particles ranging in size from 10 to 1000 nm and hold a promising role for the respiratory drug delivery [16]. Both in vitro and in vivo studies have demonstrated that nanoparticles are promising carrier systems for respiratory drug targeting, particularly to the alveoli [17–19]. However, their clinical role in respiratory tract diseases remains unclear. In bronchial asthma and COPD particularly, many researchers feel that nanoparticles may not have a role because of altogether different targeting.

We aimed to improve the efficacy of SBS DPI in the management of bronchial asthma and COPD using inhalation therapy for alveolar deposition (ITAD) concept. Our concept is based on the premise that although submicron-sized particles of SBS may not be targeted to the sites involved in bronchial asthma and COPD, yet these may possess certain advantages not associated with micro-SBS DPI.

Our work is based on three hypotheses. Micron-sized colloidal particles readily undergo phagocytosis by the macrophages stationed in the respiratory tract while nanoparticles are largely spared [20–22].This will lead to entrapment and reduction in pharmacological action of micronized drug despite being present in pharmacological quantity. The macrophages might release soluble SBS later on but the concentration by then will be too low for clinical benefit. Patients with asthma and COPD have several folds higher number of macrophages due to inflammation. Our second hypothesis was that the distally deposited nano-SBS particles will move proximally by mucociliary action and will contribute to pharmacological action at the target site. Our third hypothesis was that nano-SBS may enhance the fraction of inhaled SBS deposited in the target spaces (10–15% dose). Significantly, 60–70% of micronized SBS DPI is trapped in the pharynx, adsorbed to the much larger lactose particle. If nano-SBS could be shown to have a better respirable fraction, this could lead to more suitable pharmacokinetics.

Though in vitro methods can be used to ascertain the respiratory fraction and deposition pattern, convincing evidence can only come from DPI scintigraphy in humans. Scintigraphy offered the only way to ascertain the validity of our hypothesis that nano-SBS particles might move with the movement of mucociliary system. We recently developed a technique to chemically radiolabel SBS particle on surface using stannous ion reduction techniques [23]. DPI scintigraphy has been traditionally done by adsorbing Tc-99m DTPA on drug particle [24]. We believe that radio-chelation method possesses several advantages over simple adsorption method.

The objectives of this paper were to (a) standardize a method for making nano-salbutamol, (b) characterize the pure particle and after blending with lactose, and (c) explore possible medical advantages of nano-SBM DPI over conventional micronized SBM DPI using human scintigraphy approach.

2. Materials and methods

2.1. Chemicals

Micronised SBS (commercial) was supplied by Cipla Ltd. (Mumbai, India). Lactose (Pharmatose®) was obtained from DMV international (Veghal, The Netherlands). HPLC grade acetonitrile was purchased from Merck (India). Water used was purified by reverse osmosis (MilliQ, Millipore, USA). All others chemicals were of analytical grade.

2.2. Preparation of nano-SBS

The nano-SBS was prepared by liquid anti-solvent precipitation technique followed by spray drying. Briefly, 2.5 gm of micronized SBS was slowly dispersed in the liquid anti-solvent mixture of acetonitrile: water (70:30) under continuous magnetic stirring for 1 h at 1200 rpm. The resulting suspension was spray dried (Mini spray drier, SM Scientech SMST, Kolkata), and the conditions for spray drying were adjusted as flow rate/fed rate 91 ml/h, inlet air temperature of 75 °C and outlet air temperature of 56 °C, to obtain nano-SBS with mean particle size of 60.71 ± 35.99 nm [25].

2.3. Characterization of nano-SBS

2.3.1. Scanning electron microscopy (SEM)

SEM photographs of nano-SBS were taken by scanning electron microscope (Leo 435VP, Cambridge, UK). The samples were mounted on an aluminium stub and coated with gold in an argon atmosphere at 50 mA for 100 s using balzers SCD020 sputter coater unit (BAL-TEC GmbH, Witten, Germany).

2.3.2. Quasi-elastic light scattering (QELS)

The particle size distribution for the nanoparticles was analyzed by quasi-elastic light scattering (QELS). The prepared nanosuspension was taken in a test tube and placed in the goniometer and was analyzed by QELS, the results were recorded on the histograms.

2.3.3. Fourier transform infrared spectrometry (FT-IR)

FT-IR spectra were recorded with a FT-IR JASCO, Easton, MD spectrometer in range 400–4000 cm^{-1} using a resolution of 4 cm^{-1} and 10 scans, to evaluate the molecular states of micronized SBS and nano-SBS. Samples were mixed with potassium bromide (KBr) and were pressed to obtain supporting disks.

2.3.4. Differential scanning calorimetry (DSC)

The phase transition of micronized and nano-SBS was analyzed by differential scanning calorimeter (Pyris 6, Perkin-Elmer, USA). The DSC analysis was conducted over a heating range of 50–250 °C under controlled conditions.

2.3.5. X-ray diffraction (XRD)

The physical state of nano-SBS was studied by means of XRD patterns and compared to micronized SBS. Phase identification was conducted using an X-ray powder diffractometer (Shimadzu XRD-6000, Mumbai, India) with Cu Kα radiation at a scanning speed of 0.05°/min.

2.4. Formulation development and radiolabeling procedure

Five milligram of SBS and 495 mg of inhalation grade lactose (Pharmatose 325 M) were blended thoroughly. Each batch was prepared at a scale of approximately 500 mg. The resultant mixes were filled into hard gelatin capsules (size 3) manually so that each capsule contained 200 μg SBS.

We directly radio-complexed the surface of particulate SBS with Tc-99m using reduction technology [23]. Briefly, particulate SBS was suspended in a non-solvent containing a mix of Tc-99m pertechnetate and stannous chloride with slow stirring. After incubation of 30 min, the particulate SBS was separated out and washed a coupled of times in another non-solvent with low boiling point. A small part of the residue was analyzed for quality control using ITLC method while the major portion was dried out and passed through a sieve to break the physical aggregation. It was then weighed and blended with lactose in the desired proportion (1:67.5) and filled in gelatin capsules. In the end, the formulated capsule contained approximately 1.5–2 MBq radioactivity in the form of Tc-99m nano-SBS. A Rotahaler® (Cipla, Mumbai, India) was used as the inhalation device.

2.5. Characterization of nano-SBM DPI formulation

The aerodynamic particle deposition of SBS DPI was measured using an Anderson Cascade Impactor (ACI) (Copley Scientific, Nottingham, UK). The ACI consisted of initiation port (IP) and the preseparator (PS), seven stages and a final collection filter. The stages were coated with polypropylene glycol dissolved in hexane (2% w/w). The stages were left to dry under ambient room conditions for 1 h. Experiments were conducted at an air flow rate of 60 L min^{-1} for 4 s. The operating conditions and theoretical cut-off diameters are shown in Table 1. After actuation, the wash solutions from different parts were collected and quantitated for drug content by UV spectrophotometer.

Respirable particle fraction (RF) and emission dose (ED) were calculated to describe the inhalation properties of DPIs. The measurements were performed in six replicates.

2.6. Quality control of radiolabeled nano-SBS DPI formulation

The following procedure was done as QC of the Tc-99m SBS nanoparticle:

(a) Samples of Tc-99m SBS particles were dissolved in normal saline at different intervals till 6 hours incubation and checked for free Tc-99m pertechnetate content by ITLC method to rule out any dissociation of Tc-99m from the drug.

Table 1
Operating conditions and theoretical cut-off diameters of Anderson cascade impactor.

Anderson cascade impactor	
Flow rate (L/min)	60
Time per actuation (s)	4
Volume per actuation (L)	4
Cut-off diameter (μm)	
Stage 0	5.8
Stage 1	4.7
Stage 2	3.3
Stage 3	2.1
Stage 4	1.1
Stage 5	0.7
Stage 6	0.4
Stage 7	0.15
Stage 8	Filter

2.7. Ventilation scintigraphy with Tc-99m nano-SBM DPI

Ten healthy volunteers were recruited for ventilation scintigraphy study with Tc-99m nano-salbutamol DPI (7 males, 3 females, mean age 35 years, 22–54 years). The clinical protocol was approved by the institutional human Ethics Committee (Reg. No. INM/TS/IEC/006-017/07). Prior to dosing, subjects were trained to inhale dummy DPIs deeply and to retain the breath following deep inspiration for 10 s. The volunteers were trained to exhale into an 8-L polythene bag to collect the air expired out. Vital signs were recorded before and 30 min after each dose and before discharging the subject from the study center. Adverse events were monitored throughout the study.

The human studies were conducted on a dual head Hawkeye gamma camera system. A single gelatin capsule containing freshly prepared 1.5–2 MBq Tc-99m nano-SBM (and 200 mcg of SBM) was given to each volunteer after obtaining the radioactivity count rate of the capsule on the Gamma Camera. Upon inhalation, two-dimensional scintigraphic image of the chest region was obtained for 300 s covering the highest and lowest point of radioactivity distribution (oropharynx to stomach). It was followed by a 5-min image of the polybag containing the exhaled air. Count rate of the used capsule and the Rotacap device was found. All images were recorded on a computer system assisted with the software Entegra Version-2. Additional images of the chest were taken between 2 and 4 h. This was done to observe the movement of radioactivity if any.

Krypton-81 ventilation scan was not performed because the lung images generated by inhaled radiolabeled nanoparticles showed the lung contours prominently. Also, the main purpose of this study was to test whether the nanoparticles shifted proximally from lung spaces in time or not, which did not specifically required this additional scan.

2.7.1. Scan analysis

Images acquired on the same time scale ensured that the count statistics comparisons between different scans were valid. Region-of-Interest software was drawn around the oropharynx, esophagus, stomach, and whole lung for obtaining count statistics. The lung region was again subdivided into central, intermediate and peripheral sections which translate predominantly into respiratory tree, mixed and alveolar region, respectively [26]. The peripheral lung zone to central lung zone deposition ratio (P/C ratio) was calculated as an index of regional lung deposition. Because swallowing action continuously transports radioactivity deposited in oropharynx into stomach, counts deposited in these two organs were integrated to represent a single compartment.

Respiratory fraction, the fractions of radiolabeled drug deposited in the central, intermediate and peripheral lung, was calculated in the initial and subsequent images. Visual comparison between the lung images was done to record movement of the deposited drug with time from one compartment to another.

3. Results

3.1. Particle size, morphology and distribution

Fig. 1 details the particle size distribution analysis by QELS for nano-SBS. The mean particle size of nano-SBS prepared via liquid anti-solvent precipitation technique was 60.71 ± 35.99 nm. More than 70% particles were less than 100 nm in diameter.

SEM micrograph of the nano-SBS sample (Fig. 2) showed that nano-SBS samples were round shaped with well-defined regular morphology. Practically, no aggregation was visible between the particles. Persistence of spherical shape after several days sug-

gested lack of major interaction between the particles which would have resulted in puckering at the surface.

3.2. FT-IR analysis

The molecular states of nano-SBS were studied by means of FT-IR (Fig. 3). Close agreement between the spectra of nano-SBS with FT-IR of micronized SBS suggested that there were no changes in the structure of SBS induced by nano-sizing.

3.3. DSC and XRD analysis

DSC spectra (Fig. 4) of nano-SBS did not show any changes suggesting there was no apparent addition of impurity during the manufacturing process. The XRD patterns (Fig. 5) also suggested preservation of crystal structure in the manufacturing process. The crystalline peaks detected in the pattern of micronized SBS were also present in the XRD pattern of nano-SBS indicating that the drug is in crystalline form after precipitation.

3.4. Quality analysis of Tc-99m salbutamol sulphate nanoparticles

Radiolabeling stability. The radiolabeling efficiency at the time of complexation was 92–96% while it was 89–92% after 6 h of dry incubation. This is considered adequate for *in vivo* imaging by scintigraphy norms. Using different solvents, the amount of reduced hydrolyzed technetium was found to be 2–5%.

3.5. In vitro deposition and radiolabeling validation

The consolidated result of % drug deposition pattern of nano-SBS formulation on ACI is shown in Fig. 6 and was compared with micronized SBS, when determined spectrophotometrically by UV at 276 nm. Non-radiolabeled nano-SBS had respiratory fraction of 45.2% compared to the micronized SBS which has the respiratory fraction of 31.3%. Table 2 shows the emitted dose and dose recovery by UV method. The mean percent (SD) of total recovery for

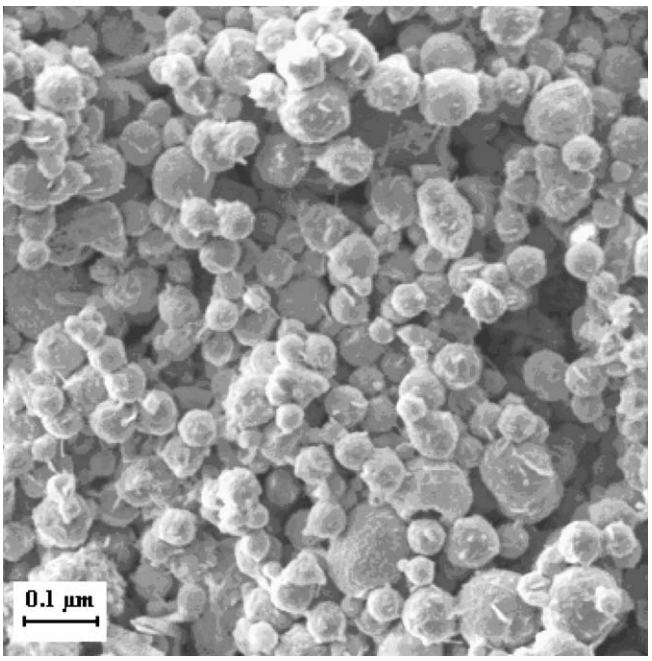

Fig. 2. SEM photomicrograph of a nano-SBS powder.

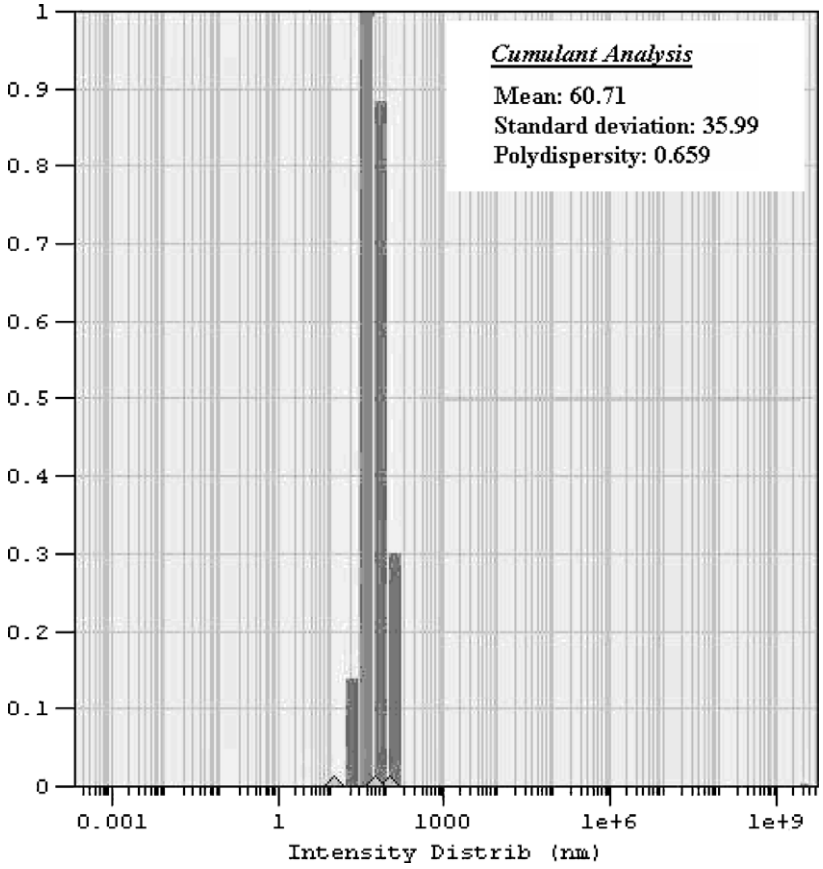

Fig. 1. Particle size distribution of Nano-SBS prepared by liquid anti-solvent precipitation followed by spray-drying technique. (Mean particle size (SD): 60 ± 35.)

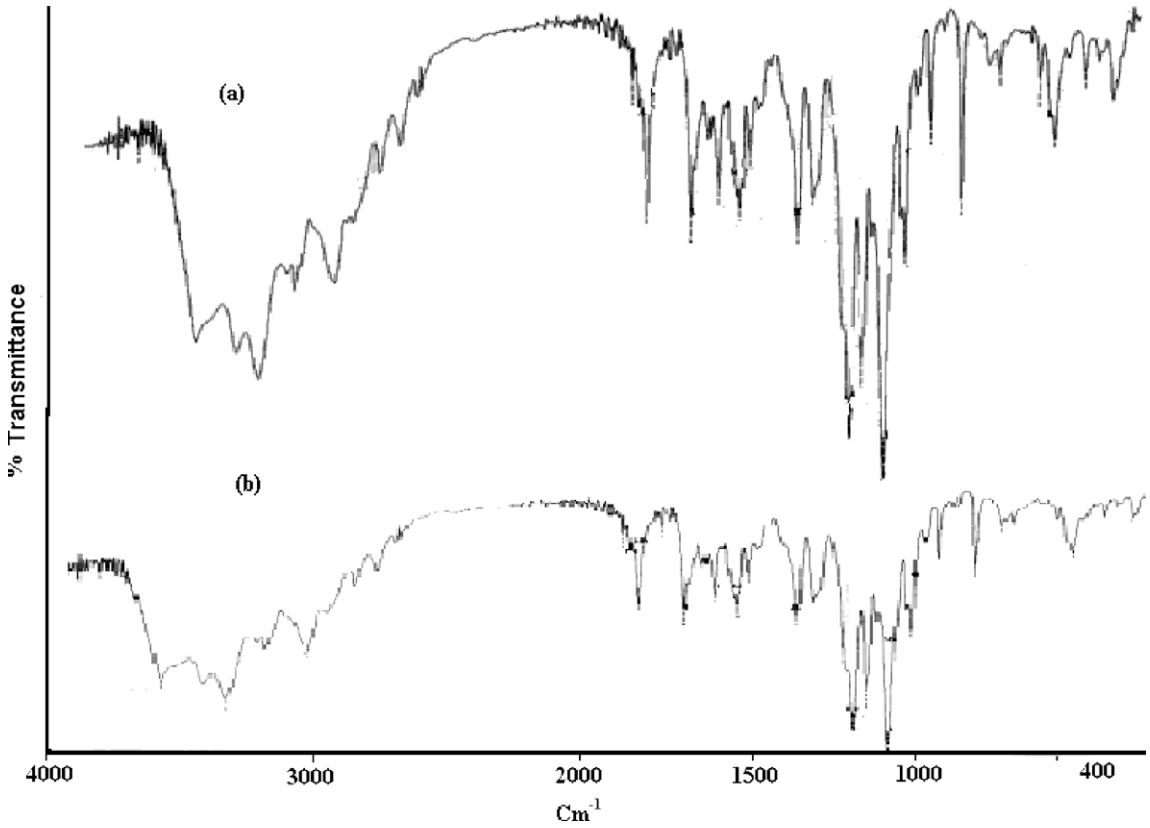

Fig. 3. FT-IR spectra of micronized SBS (a) and nano-SBS (b).

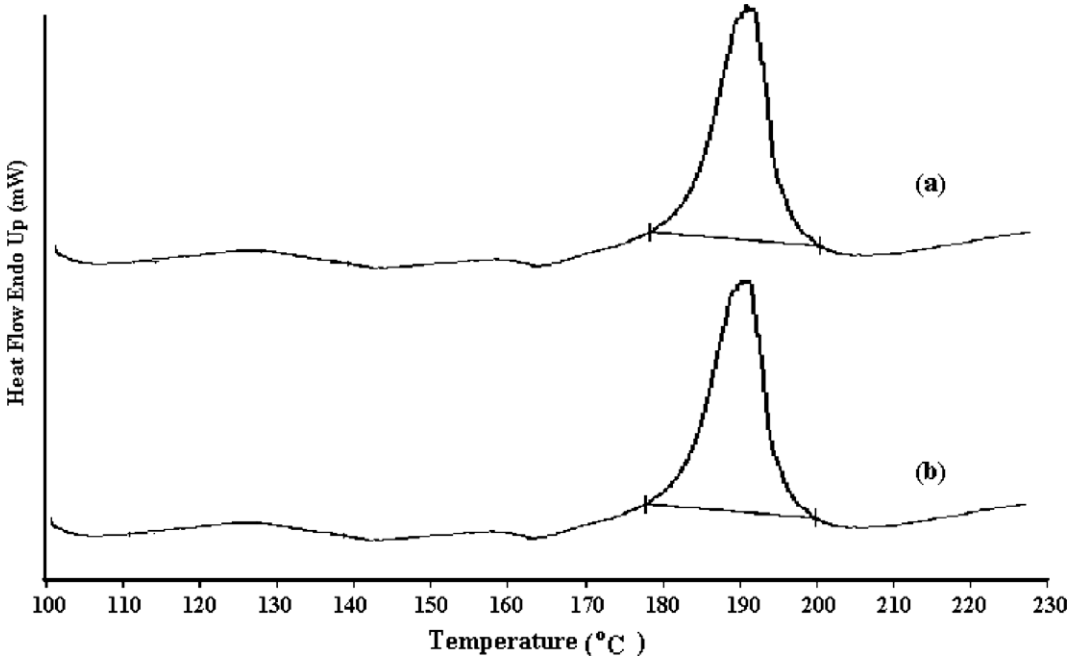

Fig. 4. Comparative thermograms of micronized SBS (a) and nano-SBS (b).

nanosized SBS formulation was 96.3% while the emitted dose was 91.3% of nominal dose delivered (200 μg).

3.6. In vivo gamma scintigraphy

No abnormal symptoms or episodes of bronchospasm were observed in the subjects during and after the study. The inhalations were well tolerated by the subjects.

The relative percentage of radiolabeled SBS dose remaining in the rotahaler, deposited in the oropharynx and lungs, and exhaled is shown in Table 3. Majority of SBS was emptied from the capsule on inhalation, with approximately 10% of the capsule dose being retained in the body of the DPI or rotahaler.

25.3 ± 4.5% of the formulation was deposited in oropharynx-stomach. The whole lung depositions averaged 64.1 ± 3.7% of the nominal dose. The remaining drug may have been transferred

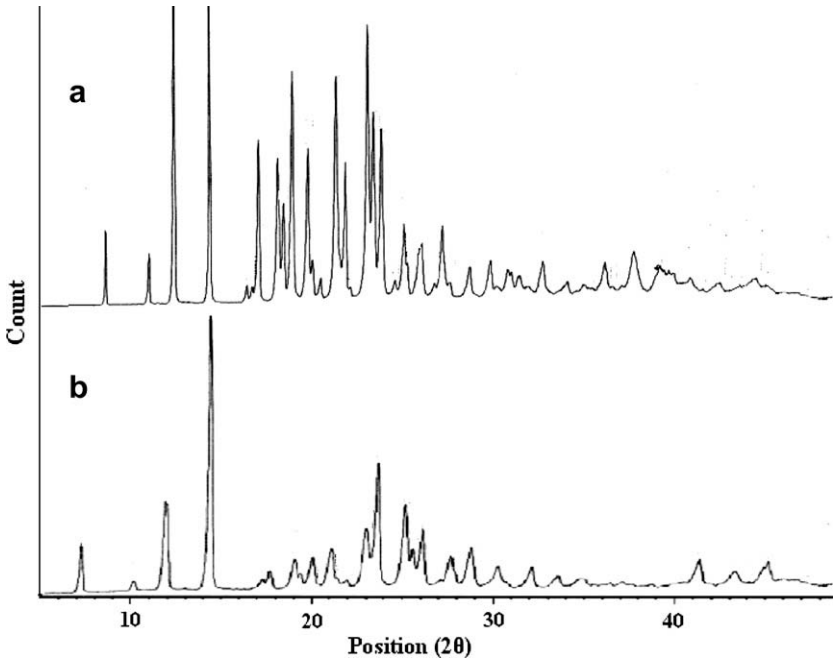

Fig. 5. Comparative XRD pattern of micronized SBS (a) and nano-SBS (b).

to the circulation. Distribution of the nano-SBS in the central, intermediate, and peripheral regions of the lung was 21–24% of the original DPI dose (Table 3). The ratio of peripheral lung zone to central lung zone deposition (P/C) was 1.2 ± 0.4. Radioactivity collected in exhalation bag was less than 1% of the emitted dose. Based on these observations, the present study suggests that about 55% of the pulmonary dose of nano-SBS reached the alveolated regions of the lung as per approximations described previously [27].

Gamma scintigraphy showed significant increase in penetration of the drug in lungs till the alveolar region with nano-SBS in comparison to micronized SBS (Fig. 7). Serial images of the lung field showed proximal movement of radioactivity deposited in lungs through the tracheo-bronchial tree. Images taken after 2–4 h post-inhalation showed reduction in lung radioactivity and increase in gastrointestinal activity. In four subjects, clear movement of tracer was seen in the later images (Figs. 8 and 9). Mathematically, deposition in peripheral lung reduced from 21% to 11%, that in tracheo-bronchial increased from 9% to 21% and radioactivity in oropharynx and stomach increased from 18% to 34% in a span of 2–4 h. The pattern suggested reversed movement of the drug from the periphery (alveolar region) to the gastrointestinal tract through the tracheo-bronchial region and oropharynx. Radioactivity in the tracheo-bronchial region increased by 50–120% in 2–4 h after DPI administration. Radioactivity was also seen in the blood pool from the early images with a rising trend suggesting that a fraction of the drug was directly transferred across the alveolar membrane to the systemic circulation.

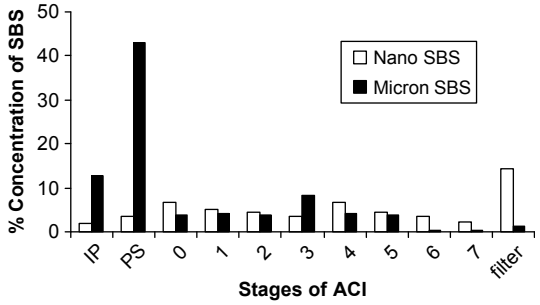

Fig. 6. ACI for % deposition profiles in each stage for nano-SBS and micronized SBS formulations showing mean (SD) percent emitted dose deposited on each stage of the ACI using Rotahaler® at 60 L min^{-1} (n = 6).

Table 2
Andersen cascade impactor (ACI) results for the DPI formulations measured using an air flow rate of 60 L min^{-1} (n = 6).

Particle size attributes	ACI (inhalation indices)	
	Nano-SBS	Micronized SBS
Emitted dose (%)	91.3 ± 3.20	90.8 ± 2.90
Respiratory fraction [a] (%)	45.2 ± 5.20[b]	31.3 ± 3.10
Total recovery	96.3 ± 1.18	97.2 ± 2.38
Mean Median Aerodynamic diameter (μm)	1.61 ± 0.01	3.08 ± 0.04

[a] Respiratory fraction calculated as ratio of total drug deposited in the lower stages of the ACI (stages 2–8) to total theoretical dose.
[b] $P < 0.001$ vs. micronized SBS.

Table 3
Regional deposition of radiolabeled nano-SBS and micronized SBS formulation.

	Percent (%) of nominal dose Mean ± SD	
n = 10[a]	Nano-SBS	Micronized SBS
Capsule	02.1 ± 1.4	02.3 ± 1.2
Rota inhaler	08.6 ± 2.1	10.0 ± 3.2
Emitted dose	89.1 ± 2.8	87.7 ± 5.6
Oropharynx[b]	25.3 ± 4.5[c]	58.4 ± 6.1
Whole lung	64.1 ± 3.7[d]	28.3 ± 5.2
Central lung	20.0 ± 2.7[c]	10.9 ± 1.8
Intermediate lung	21.3 ± 3.1[c]	08.7 ± 1.6
Peripheral lung	22.6 ± 2.4[c]	08.9 ± 1.5
Exhalation filter	0.1 ± 0.1	0.0 ± 0.0

[a] Data shown are from the 10 subjects who completed the study.
[b] The oropharynx includes deposition in the mouth, pharynx, esophagus, stomach, and intestine.
[c] $P < 0.05$ vs. micronized SBS.
[d] $P < 0.001$ vs. micronized SBS.

4. Discussion

In this study, the hypothesis that nano-SBS DPI may have better distribution characteristics and may be a better treatment option compared to the micronized form was tested. A novel nano-SBS DPI formulation was developed, characterized, and its deposition pattern, including in vivo deposition in humans, was examined. In this respect, the human study served as a zero-phased human trial. The major information elicited on nano-SBS included (a) smooth rounded 60 nm sized particles that showed no impurity or change in crystalline nature during manufacture, (b) some tendency for interparticle adhesions when in close contact with each other in dry state, (c) significantly reduced interaction with lactose compared to micro-SBS DPI resulting in near-doubling of respiratory fraction (confirmed on ACI and human data), (d) significantly higher fine particle distribution, with lung deposition more than 50% of the inhaled dose (estimated on scintigraphy), and perhaps most importantly, (e) demonstration of reverse movement of radiolabeled nano-SBS deposited in the lungs through mucociliary system back to tracheo-bronchiolar area. In the human studies, delayed images suggested up to 130% enhancement of nano-SBS concentration in the target area compared to the initial deposition after a single inhalation.

In absolute terms, considering the loading dose of 200 mcg SBS in DPI capsules and emitted dose of 90%, the dose deposited in the tracheo-bronchial region in the initial phase estimated by scintigraphy was 18 mcg going up to 40 mcg by 2–4 h. Micro-SBS deposition in the target is described as 5–15% of the inhaled dose [8], which is 10–30 mcg with a 200 mcg dose, but rapidly deteriorates thereafter, as manifested by the need for very frequent dosing. Nano-SBS, on the other hand, has an equivalent drug concentration in the initial phase continued till at least 2–4 h the period for which the study was conducted. Thus, the results suggest higher local bioavailability for a significantly longer period of time with nano-SBS compared to micro-SBS DPI using the same inhaled drug dose. The reason for this advantage, as hypothesized in the beginning, is the significantly higher respiratory fraction and fine particle fraction that results in equivalent or higher local bioavailability at the target site in the beginning, sustained by the movement of particles deposited in the lungs into the target area. This advantage is not available with microparticles. Apart from the more sustained action on the large bore respiratory tract (exemplified by trachea and primary bronchi), nanoparticles are likely to be more effective in constrictive diseases of the small bore respiratory conduits, exemplified by secondary and tertiary bronchioles, and in the presence of tortuous and fluid-filled respiratory tracts. Nanoparticles show delayed lung clearance [8]. These advantages suggest that the role of SBS DPI can be extended from primarily a preventive role to a therapeutic option in moderate-to-severe bronchial asthma and COPD by reducing the size of the aerosol and redefining the optimum MMAD. In accordance with the findings of Usmani et al. [28], it is therefore very much likely that smaller particles give notably greater bronchodilation. A spin-off advantage of reduced oropharyngeal deposition of SBS is less likelihood of systemic side-effects like tachycardia and increased tendency of esophagitis.

In previous studies, researchers have investigated the relationships between mass median aerodynamic diameter (MMAD) and aerosol lung deposition [14,29,30]. However most have dealt with small particle with MMAD reduced to 1–2 μm. Very few reports deal with submicronic or nano-SBM, particularly because smaller particles are expired off contributing to reduced pharmacological and clinical action. Our study shows that nano-SBS can be manufactured in ways that can result in greater adhesion with the lung parenchyma and have lower interaction with lactose vehicle. Micronized drug often comprises of flat surfaces. As a result, the area of contact between particles is large and the attractive forces with lactose can be strong. The area of contact between spherical particles is less than that is found for flat surfaces, and often results in a very weak interaction [31]. Carrier particles in interactive mixtures may form agglomerates with drug and deposit in the proximal airways [32]. Normally, two-third of inhaled micronized particles travel to the gastrointestinal tract (or IP & PS in the ACI) due to adhesion to the lactose vehicle. With nano-SBS particles, the fraction adhering to lactose was 30% on ACI and 25% in the human scintigraphy study. We have seen the same pattern, i.e., increase in respirable fraction, in the case of other nanoparticles we have made, such as atropine sulphate, fluticazone and calcium edentate. The reason of reduced interaction with lactose can probably be traced to smoother surface and the fact that rotational spin imparted by inspiration (or by ACI motor) is likely to disengage lighter nanoparticles to a greater extent than microparticles that are 10–100 times heavier, consistent with the principle of centrifugal forces. The same observation has been reported previously [33], though we could not measure the surface energy of the particles, the results of this study suggest that it will be lower than that of the microparticles. The improvement in lung penetration noted with nano-SBS powder may also be the result of several factors which influence the interparticle separation distance, or the area of contact between particles [34].

On SEM, nano-SBS particle size was 60 nm while on laser optimetry and ACI, the mean particle size was close to 100 nm and 130 nm, respectively. Though different instruments were used to measure particle size in different situations, the pattern of increasing particulate size suggests that interaction between nanoparticles themselves is enhanced. The data suggest that aggregation is taking place as the particles are dried and blended with lactose, or even thereafter. It may be inferred that unless these particles are separated by preponderant lactose particles, these shall interact amongst themselves with a much greater attractive force. This phenomenon has implications for the storage of the nano-formulations. The number of drug particles blended in the vehicle shall play an even more important role in the aggregation of nanoparticles because for the same amount of the drug (200 mcg), the number of nanoparticles will be significantly higher than microparticles, giving a greater probability of proximity and interaction. In the case of nano-salbutamol, the initial size of particles

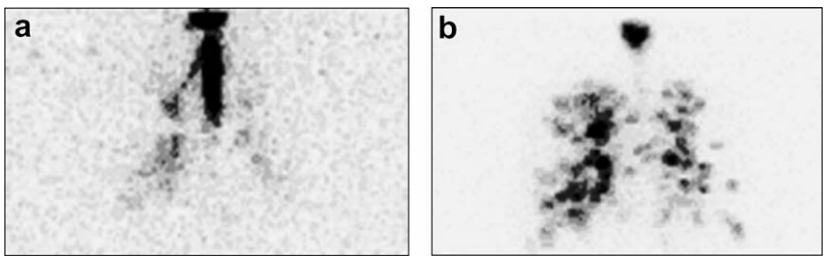

Fig. 7. Gamma scintigraphic image showing micronized SBS (a) and nano-SBS (b).

was 60 nm. Assuming spherical shape and equal drug density in both types of particles (and taking 5 μm as the size of micronized salbutamol), for every microparticle there will be 5.8×10^8 nanoparticles.

Humidity, for the same reason shall play a more critical role in the case of nano-SBS even if SBS is not particularly hygroscopic. Though the data are as yet not statistical, the shelf life of our formulation at present may not be more than 3 months, which is

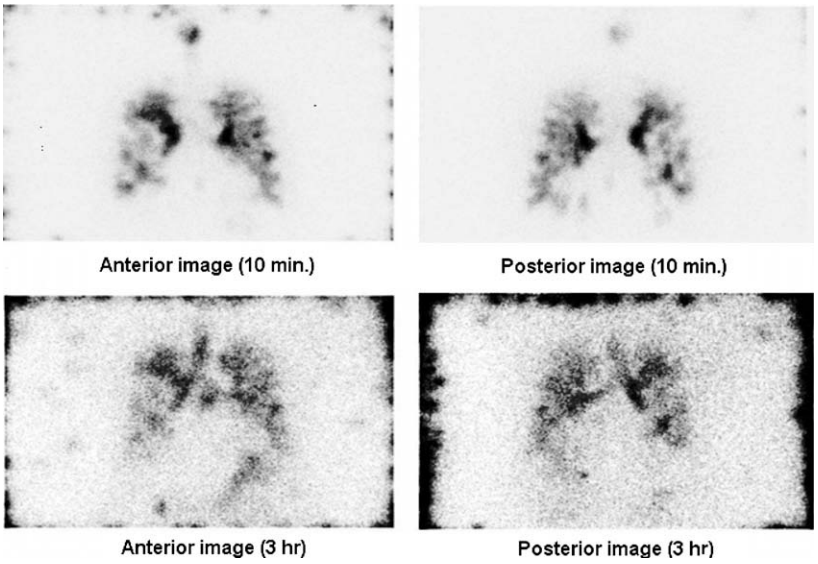

Fig. 8. Ventilation scan with Tc-99m nano-SBS DPI: anterior and posterior lung Image at 10 min post-inhalation shows initial distribution pattern of radiolabeled SBS nanoparticles (upper images). Note the absence of radioactivity in stomach. Image taken after 3 h (lower images) shows proximal movement of the radiolabeled drug, visualization of trachea-primary bronchi, and increased drug concentration in stomach. The pattern is consistent with mucociliary movement of the drug.

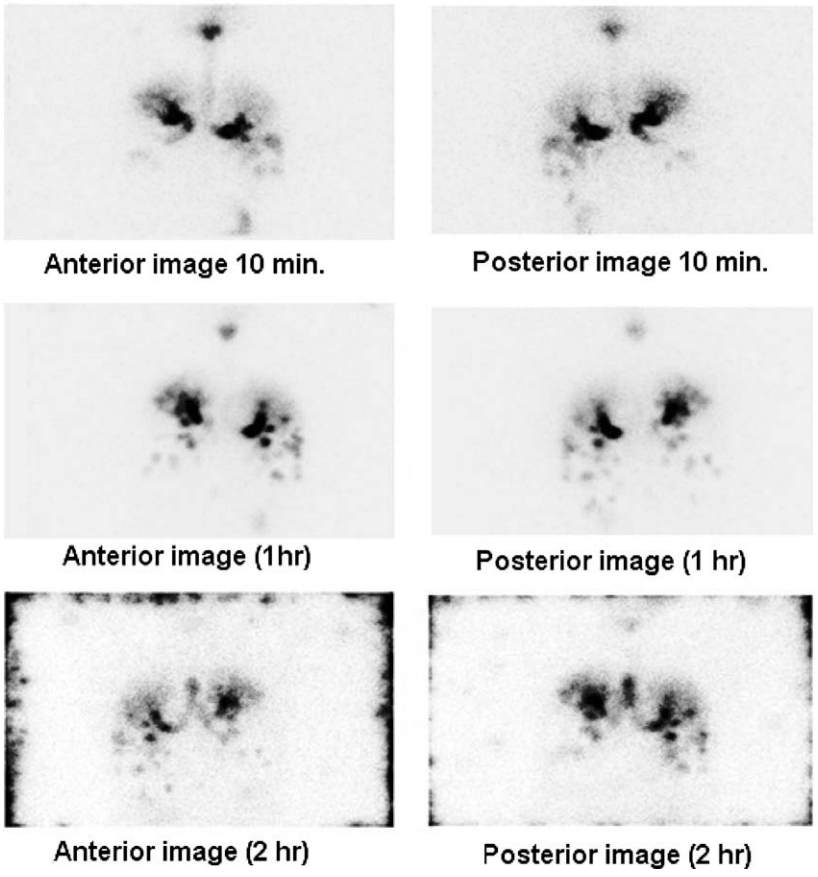

Fig. 9. Anterior and posterior lung visualization by ventilation scan with Tc-99m nano-SBS DPI at 10 min (upper images, 1 h (middle images) and 2 h (lower images). The study shows the changing distribution pattern of radiolabeled SBS nanoparticles with time. The radiolabeled drug slowly moves out from the lung spaces proximally. Delayed images show clear visualization of drug draining from the primary bronchi into the trachea.

clearly unacceptable. We are trying to enhance the shelf life using several methods, including the replacement of conventional gelatin capsules that are relatively hygroscopic, by cellulose-based capsules.

Clinical efficacy of inhaled submicronic particles is supposed to be low due to higher expiration rate [15]. However, our experiments showed 1% exhalation of radioactive nanoparticles into the collection bag. This was reconfirmed on serial scintigraphy when lung deposition was found to be around 50% of the inhaled dose and about 90% drug accounted for in the in vivo distribution (at 10 min post-inhalation). Even in the delayed phase, the missing counts, presumed to have been lost to exhalation, were less than 8% in all cases. It appears that the manufacturing process is the critical factor, responsible for greater interaction and adhesion of the nano-drug with the alveolar membrane. The crucial process parameters may include the stirring rate, concentration of drug and the volume ratio of solvent to non-solvent (data not shown). Dry milling and spray drying often produce amorphous materials, which are hygroscopic, cohesive, poorly dispersed and thermodynamically unstable. The drug particles described in the present study showed crystalline peaks of high intensities indicating high crystallanity and greater stability.

Scintigraphy has been valuable in reaching several of the conclusions in the study. Instead of using conventional Tc-99m DTPA adsorption described in the literature [24], we developed a method to directly label salbutamol sulphate particles with Tc-99m by means of surface labeling [23] ensuring true representation of the deposition pattern. We believe Tc-99m DTPA adsorption method may lead to inaccuracies. In, *in vitro* experiments with air jet (saturated with water vapor) sprayed over such a formulation before passing through appropriate meshes; we were able to demonstrate significant transfer of the radiolabel to the lactose (unpublished data). Though many studies have shown equivalence of radioadsorbed SBS with particulate SBS in, *in vitro* procedures, it is more likely for the adsorbed radioactivity on the surface of particulate SBS to transfer too much more ubiquitous lactose or to dissolve in the liquid phase in the capsule and human body, respectively. On the other hand, a fraction of dry molecular radioactivity (Tc-99m DTPA) is likely to spill off the much bigger SBS particle during inspirational pull due to the air currents, similar to detachment of SBS particles from the much bigger lactose in the same act. The former shall overestimate and the latter shall under-report the functional particle size in vivo.

Another feature of scintigraphy in this study was the non-use of Xenon-131 or Krypton-81 ventilation scan image. The gases have been frequently used in defining the micronized DPI distribution by delineating the lung silhouette. However, since we used nanoparticles which penetrate the lung till the alveolar region (Fig. 7), the whole lung morphology becomes quite obvious, obviating the need for an additional Xenon-131 or Krypton-81 superimposition image. This is significant considering the fact that these gases are not available in most nuclear medicine centers and limit DPI experimentation. We did not use attenuation correction because attenuation was a constant and, therefore, not a factor in determining the distribution profile and dynamics of the deposited particles.

Though radiolabeling did not change the size of nanoparticles as measured on SEM, there was small but definitive increase in size on laser optometry and ACI suggesting aggregation of particles. However, the increase was about 10%, which is quite acceptable in assessing the in vivo distribution of particles. There was a good correlation between deposition pattern of the labeled and unlabeled nano-SBS formulation on ACI, and deposition analysis of the drug particles can be made still more accurate by using renormalization factor for each stage of the ACI. As part of phase-2 efficacy study, we are now studying the effect of the formulation on pulmonary function test and exercise performance of mild and moderately severe cases of bronchial asthma and COPD, along with nanoparticle ventilation scanning acting as a response-predictor in individual cases.

It is concluded from the study that (a) nano-SBS particles can be generated which possess capability of higher interaction with the lung membrane, (b) it may represent a novel method of treating bronchial asthma and COPD by virtue of significantly higher peripheral deposition and mucociliary movement back to trache-o-bronchial region causing higher and more sustained drug concentration in the target area, and (c) surface labeling of SBS particles is a better method than Tc-99m DTPA adsorption method for DPI characterization.

Appendix A. Supplementary data

Supplementary data associated with this article can be found, in the online version, at doi:10.1016/j.ejpb.2008.09.018.

References

[1] G. Braganza, N.C. Thomson, Acute severe asthma in adults, Adult Asthma (2008) 209–212.
[2] N. Khaltaev, E. Minelli, P. Desloovere, Global alliance against chronic respiratory diseases (GARD): a world where all people breathe freely, Revue franc¸aise d'allergologie et d'immunologie clinique 47 (2007) 246–247.
[3] R.G. Boltea, Emergency department management of pediatric asthma, Clin. Pediatric Emerg. Med. 5 (4) (2004) 256–269.
[4] J.W. Georgitis, The 1997 Asthma management guidelines and therapeutic issues relating to the treatment of asthma, Chest 115 (1999) 210–217.
[5] M.T. Newhouse, K.J. Corkery, Aerosols for systemic delivery of macromolecules, Respir Care Clin. N. Am. 7 (2001) 261–275.
[6] W.D. Bennett, J.S. Brown, K.L. Zeman, S.C. Hu, G. Scheuch, K. Sommerer, Targeting delivery of aerosols to different lung regions, J. Aerosol Med. 15 (2002) 179–188.
[7] R. Dhand, Future directions in aerosol therapy, Respir. Care Clin. N. Am. 7 (2001) 319–335.
[8] S. Schurch, P. Gehr, V.I. Hof, M. Geiser, F. Green, Surfactant displaces particles towards the epithelium in airways and alveoli, Respir. Physiol. 80 (1990) 17–32.
[9] G. Caramori, I. Adcock, Pharmacology of airway inflammation in asthma and COPD, Pulmonary Pharmacol. Ther. 16 (2003) 247–277.
[10] P.M. Young, D. Cocconi, P. Colombo, R. Bettini, R. Price, D.F. Steele, M.J. Tobyn, Characterization of a surface modified dry powder inhalation carrier prepared by "particle smoothing", J. Pharm. Pharmacol. 54 (10) (2002) 1339–1344.
[11] M. Wedaa, P. Zanenb, A.H. de Boerc, D.M. Barendsa, H.W. Frijlinkc, An investigation into the predictive value of cascade impactor results for side effects of inhaled Salbutamol, Int. J. Pharm. 287 (1–2) (2004) 79–87.
[12] K.A. Johnson, Preparation of peptide and protein powders for inhalation, Adv. Drug Deliv. Rev. 26 (1997) 29–40.
[13] H. Schulz, Mechanisms and factors affecting intrapulmonary particle deposition: implications for efficient inhalation therapies, Pharm. Sci. Technol. Today 1 (1998) 336–344.
[14] E. Bondesson, T. Bengtsson, L. Borgstrom, L.-E. Nilsson, K. Norrgren, E. Trofast, P. Wollmer, Planar gamma scintigraphy-points to consider when quantifying pulmonary dry powder aerosol deposition, Int. J. Pharm. 251 (2003) 33–47.
[15] J.C. Sung, B.L. Pulliam, D.A. Edwards, Nanoparticles for drug delivery to the lungs, Trends Biotechnol. 25 (12) (2007) 563–570.
[16] J. Kreuter, Drug targeting with nanoparticles, Eur. J. Drug Metab. Pharmacol. 19 (1994) 253–256.
[17] P. Couvreur, C. Vauthier, Polyalkylcyanoacrylate nanoparticles as drug carrier: present state and perspectives, J. Control. Release 17 (1991) 187–198.
[18] J. Kreuter, Nanoparticle-based drug delivery systems, J. Control. Release 16 (1991) 169–176.
[19] B.Y. Shekunov, P. Chattopadhyay, H.H.Y. Tong, A.H.L. Chow, Particle size analysis in pharmaceutics: principles, methods and applications, Pharm. Res. 24 (2007) 203–226.
[20] A.O. Fels, Z.A. Cohn, The alveolar macrophage, J. Appl. Physiol. 60 (1986) 353–369.
[21] D.A. Edwards et al., Recent advances in pulmonary drug delivery using large, porous inhaled particles, J. Appl. Physiol. 85 (1998) 379–385.
[22] G. Oberdorster et al., Nanotoxicology: an emerging discipline evolving from studies of ultrafine particles, Environ. Health Perspect. 113 (2005) 823–839.
[23] G. Mittal, T. Singh, N.C. Gooomer. A. Bhatnagar, A. Lulla, G. Malhotra, R. Kashyap, R.P. Tripathi, Formulations and methods thereof for making Radiolabeled Dry Powder, Patent No. 1536/DEL/2008.
[24] G. Pilcer, J. Goole, B.V. Gansbeke, D. Blocklet, C. Knoop, F. Vanderbist, K. Amighi, Pharmacoscintigraphic and pharmacokinetic evaluation of tobramycin DPI formulations in cystic fibrosis patients, Eur. J. Pharm. Biopharm. 68 (2008) 413–421.

[25] M. Bhavna, F.J. Ahmad, R.K. Khar, S. Sultana, A. Bhatnagar, Techniques to develop and characterize nanosized formulation for salbutamol sulfate, J Mater Sci Mater Med. 10 June 2008 [Epub ahead of print].
[26] S.P. Newman, A.R. Clark, N. Talalee, S.W. Clarke, Pressurised aerosol deposition in the human lung with and without an open spacer, Thorax 44 (1989) 706–710.
[27] L. Borgstrom, E. Bondesson, F. Moren, E. Trofast, S.P. Newman, Lung deposition of budesonide inhaled via Turbuhaler: a comparison with terbutaline sulphate in normal subjects, Eur. Respir. J. 7 (1994) 69–73.
[28] O.S. Usmani, M.F. Biddiscombe, P.J. Barnes, Regional lung deposition and bronchodilator response as a function of beta2-agonist particle size, Am. J. Resp. Crit. Care Med. 172 (2005) 1497–1504.
[29] J. Nazir, D.J. Barlow, M.J. Lawrence, C.J. Richardson, I. Shrubb, Artificial neural network prediction of aerosol deposition in human lungs, Pharm. Res. 19 (8) (2002) 1130–1136.
[30] J. Nazir, M.J. Lawrence, I. Shrubb, Artificial neural network prediction of the patterns of deposition of polydisperse aerosols within human lungs, J. Pharm. Sci. 94 (9) (2005) 1986–1997.
[31] H. Schiavone, S. Palakodaty, A. Clark, P. York, S.T. Tzannis, Evaluation of SCF-engineered particle-based lactose blends in passive dry powder inhalers, Int. J. Pharm. 281 (2004) 55–66.
[32] F. Podczeck, The influence of particle size distribution and surface roughness of carrier particles on the in vitro properties of dry powder inhalations, Aerosol Sci. Tech. 31 (1999) 301–321.
[33] N. Nantel, M.T. Newhouse, Inspiratory flow rates through a novel dry powder inhaler (Clickhaler) in pediatric patients with Asthma, J. Aerosol Med. 12 (2) (1999) 55–58.
[34] R.O. Williams III, J. Brown, J. Liu, Influence of micronization method on the performance of a suspension triamcinolone acetonide pressurized metered-dose inhaler formulation, Pharm. Dev. Technol. 4 (2) (1999) 167–169.